RESEARCH ARTICLE

PHYSICS

Double-frequency Aharonov-Bohm effect and non-Abelian braiding properties of Jackiw-Rebbi zero-mode

Yijia Wu[1], Haiwen Liu[2], Jie Liu[3,*], Hua Jiang[4] and X.C. Xie[1,5,6,*]

[1]International Center for Quantum Materials, School of Physics, Peking University, Beijing 100871, China; [2]Center for Advanced Quantum Studies, Department of Physics, Beijing Normal University, Beijing 100875, China; [3]Department of Applied Physics, School of Science, Xi'an Jiaotong University, Xi'an 710049, China; [4]School of Physical Science and Technology, Soochow University, Suzhou 215006, China; [5]Beijing Academy of Quantum Information Sciences, Beijing 100193, China and [6]CAS Center for Excellence in Topological Quantum Computation, University of Chinese Academy of Sciences, Beijing 100190, China

*Corresponding authors. E-mails: jieliuphy@xjtu.edu.cn; xcxie@pku.edu.cn

ABSTRACT

Ever since its first proposal in 1976, Jackiw-Rebbi zero-mode has been drawing extensive attention for its charming properties including charge fractionalization, topologically protected zero-energy and possible non-Abelian statistics. We investigate these properties through the Jackiw-Rebbi zero-modes in quantum spin Hall insulators. Though charge fractionalization is not manifested, Jackiw-Rebbi zero-mode's zero-energy nature leads to a double-frequency Aharonov-Bohm effect, implying that it can be viewed as a special case of Majorana zero-mode without particle-hole symmetry. Such relation is strengthened for Jackiw-Rebbi zero-modes also exhibiting non-Abelian properties in the absence of superconductivity. Furthermore, in the condition that the degeneracy of Jackiw-Rebbi zero-modes is lifted, we demonstrate a novel non-Abelian braiding with continuously tunable fusion rule, which is a generalization of Majorana zero-modes' braiding properties.

Keywords: Jackiw-Rebbi zero-mode, Aharanov-Bohm effect, non-Abelian statistics, Majorana zero-mode

INTRODUCTION

Jackiw-Rebbi zero-mode was first raised as the zero-energy soliton solution of Dirac equation in one spatial dimension [1]. In the presence of such a zero-mode, the total charge of the 'Dirac sea' is half-integer [2–6] due to charge-conjugation symmetry, which is regarded as another mechanism of charge fractionalization, in addition to the prestigious fractional quantum Hall (FQH) effect [7–10]. In condensed matter physics, Jackiw-Rebbi zero-mode is closely related to the band topology [11,12]. The first famous example is the Su-Schrieffer-Heeger (SSH) model [13] whose low-energy effective Hamiltonian is equivalent to a 1D topological insulator (TI), and Jackiw-Rebbi zero-mode resides in the domain wall separating topologically distinct phases. Another celebrated example is the Kitaev's chain [14] whose effective Hamiltonian is again equivalent to a 1D TI. The difference is that the zero-mode here is self-conjugate due to the superconductivity and therefore a Majorana one. In this vein, Jackiw-Rebbi zero-mode can be regarded as a special case of Majorana zero-mode (MZM) in the absence of particle-hole (PH) symmetry [10,15].

In the last decade, Jackiw-Rebbi zero-mode was proposed in topological systems including spin ladders [16,17], Rashba nanowires [18–21], and quantum spin Hall insulator (QSHI) with constriction [22,23] or external magnetic field [24]. These zero-modes are created or annihilated pairwisely, hence the braiding processes are non-commutative [8] due to the fermion parity conservation [16,25]. However, on the contrary of its Majorana cousin [26], Jackiw-Rebbi zero-mode's non-Abelian nature has not yet been demonstrated in a practical device such as trijunction [17,27–30] or cross-shaped junction [31,32] as has been done for MZMs.

Another peculiar property of the Jackiw-Rebbi zero-mode is the 1/2 charge fractionalization, which has been claimed [24] to be detectable in a pumping process [33] or by Coulomb blockade. Recently, a novel 3/2 FQH plateau is observed in single layer 2D electron gas with confined geometry [34]. Jackiw-Rebbi zero-mode induced by the confined geometry could be a tentative explanation [34] that similar mechanism has been proposed in QSHI [22].

In this article, we first construct a QSHI heterostructure supporting Jackiw-Rebbi zero-mode. Then we investigate the Aharonov-Bohm (AB)
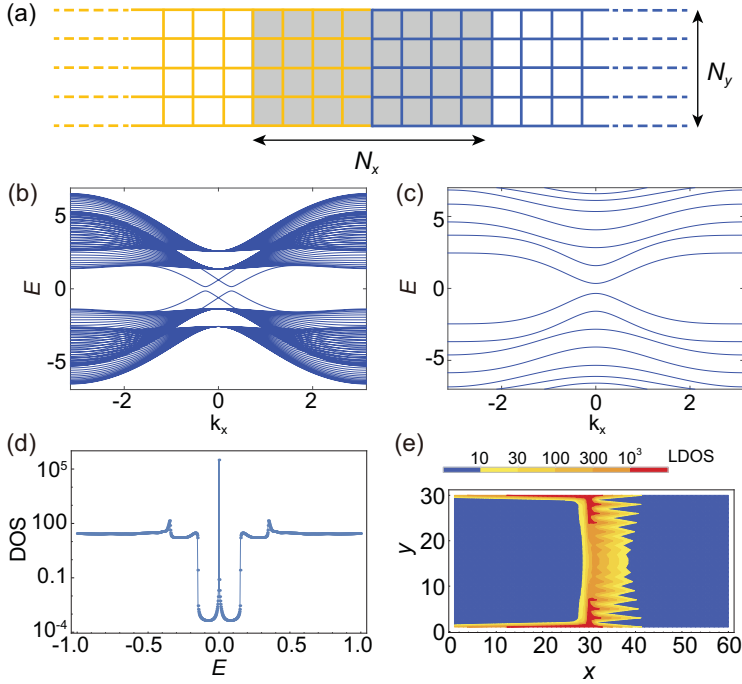
Figure 1. (a) Schematic diagram of the QSHI heterostructure lattice [with finite width $N_y = 30$ through (a-e)] which is composed of two semi-infinite QSHI halves (yellow and blue, respectively) whose energy spectrums are shown as (b) and (c), respectively. Hamiltonian parameter $A_y = 2$ in (b) and there are four edge channels; $A_y = 40$ in (c) and the edge channels here are destroyed. (d) The DOS inside the shaded region ($N_x = 60$) of (a). (e) The local density of states distribution inside the shaded region of (a) at energy $E = 0$. Other parameters are $A_x = 2.2$, $B = 1$, $M = 2$, $\Delta_z = 0.6$, and $\Delta_x = 0.15$.

effect where a single Jackiw-Rebbi zero-mode is embedded in an AB ring, showing a double-frequency AB oscillation at zero-energy. A comparison with MZM's AB effect supports the aforementioned relation between Jackiw-Rebbi zero-mode and MZM. We also set up a cross-shaped QSHI junction and numerically confirm the non-Abelian braiding properties of Jackiw-Rebbi zero-modes to be in analogy with MZMs. Importantly, Jackiw-Rebbi zero-modes represent a novel non-Abelian braiding corresponding to a generalized fusion rule when the zero-modes' degeneracy is lifted by chiral-symmetry-breaking disorder or by tuning gate voltages. Such generalized and continuously tunable non-Abelian braiding can also be realized for MZMs if 'fictitious' disorder breaking PH-symmetry is presented.

LATTICE REALIZATION OF JACKIW-REBBI ZERO-MODE

The 1D effective Hamiltonian describing four edge channels of QSHI constriction can be constructed [22] as $H_{1D} = v_F\ \hat{p}_x\rho_z\tau_0 + \Delta_x\rho_x\tau_0 + \Delta_z\rho_z\tau_z + t\rho_x\tau_x$, where the four terms represent the kinetic

energy, the spin-orbit interaction (SOI), the Zeeman term, and a spin-conserved inter-edge tunneling term, respectively (ρ_i, τ_i are Pauli matrices working in right-/left-moving spinor and chirality spinor, respectively). The competition between the Zeeman term Δ_z and the tunneling strength t induces two distinct topological phases and the Jackiw-Rebbi zero-mode resides in the domain wall. The effective Hamiltonian $H_{eff} = (\Delta_x/t)p_x\pi_x + (\Delta_z - t)\pi_z$ describing topological phase transition has the form of 1D TI (π_i are Pauli matrices for real spin). It is worth noting that quantum Hall insulator with two pairs of edge channels [34] possesses similar Hamiltonian.

The 2D Hamiltonian of QSHI constriction supporting Jackiw-Rebbi zero-modes is obtained by adding the Zeeman term Δ_z and the SOI term Δ_x into the Bernevig-Hughes-Zhang (BHZ) model [35,36] as:

$$H_{QSHI}(\mathbf{p}) = \begin{pmatrix} h(\mathbf{p}) + \Delta_z\sigma_0 & \Delta_x\sigma_0 \\ \Delta_x\sigma_0 & h^*(-\mathbf{p}) - \Delta_z\sigma_0 \end{pmatrix}, \quad (1)$$

where $h(\mathbf{p}) = (A_x p_x\sigma_x - A_y p_y\sigma_y) + (M - B\mathbf{p}^2)\sigma_z$ (σ_i for Pauli matrices). The discretized version of Equation (1) in a 2D lattice with finite width N_y generally possesses four edge states. However, a strong inter-edge tunneling will destroy these edge states and bring about a topologically trivial phase. The strength of such tunneling depends on the overlap between opposite edge states, therefore it can be modulated through the Hamiltonian parameters [e.g., A_y, see Fig. 1(b, c)] or lattice width N_y (i.e., QSHI constrictions [22,23]). Based on the method of Green's function, the density of states (DOS) [Fig. 1(d, e)] of a QSHI heterostructure [Fig. 1(a)] composed of two topologically distinct halves demonstrates the subgap zero-energy Jackiw-Rebbi state localized at its interface. It is worth noting that the Jackiw-Rebbi zero-mode's energy may deviate from zero [e.g. if kinetic term $(C - D\mathbf{p}^2)$ is presented in the BHZ model]. However, both the transport and the braiding properties of the Jackiw-Rebbi zero-modes remain unchanged in the presence of such a constant shift of energy.

THE AHARONOV-BOHM EFFECT OF JACKIW-REBBI ZERO-MODE AND A COMPARISON WITH MZM

Apart from pumping of the domain wall [24,33], transport signature of Jackiw-Rebbi zero-mode is also shown in the Jackiw-Rebbi zero-mode intermediated electron transmission [18,37],
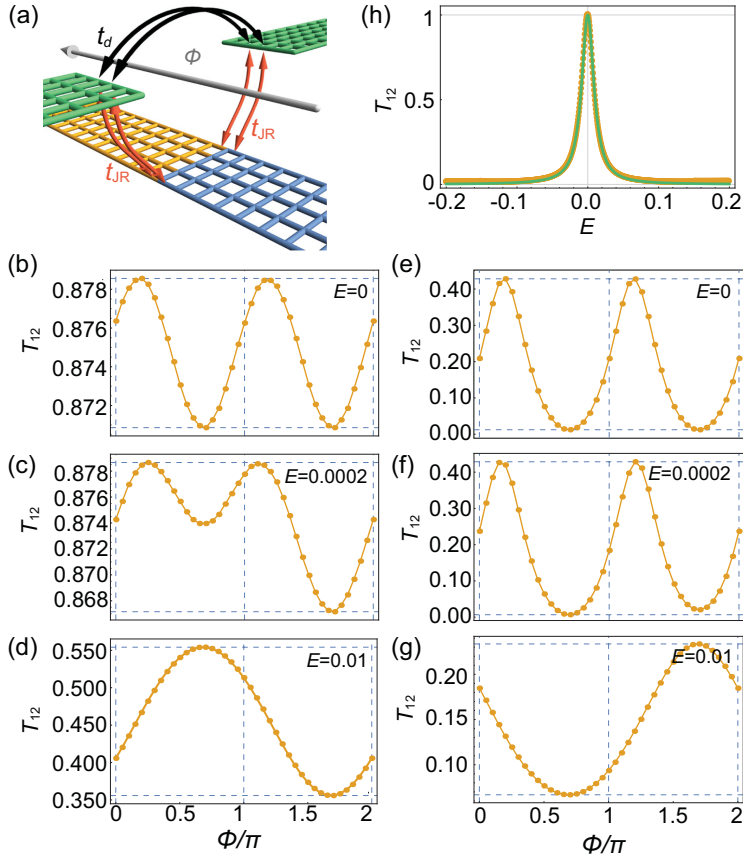
Figure 2. (a) Sketch of the AB ring in a lattice model. An AB ring enclosing a magnetic flux ϕ is sandwiched between two identical 2D metal leads (green lattice). The upper arm of the ring is the direct hopping with strength t_d between the two leads (black arrows), and the lower arm contains a Jackiw-Rebbi zero-mode in a QSHI heterostructure (yellow and blue lattice) which is equally coupled to the two leads with hopping strength t_{JR} (orange arrows). (b-d) [(e-g)] In the condition of weak (strong) t_d, numerical results of T_{12} at fixed energies as (b) [(e)] $E = 0$, (c) [(f)] $E = 0.0002$, and (d) [(g)] $E = 0.01$, respectively. For simplicity, in (b-g), conductance constants irrelevant to the oscillations have been subtracted. (h) T_{12} solely induced by the Jackiw-Rebbi zero-mode, where numerical results (orange) can be perfectly fitted by the analytic formula (green) with $\tilde{E} \approx 95 E$.

whose peculiarities may be revealed by a two-path interference with a normal electron transmission, i.e., AB effect with a Jackiw-Rebbi zero-mode embedded [Fig. 2(a)]. The direct hopping strength between the two leads is t_d, and the hopping strength between the leads and the QSHI heterostructure supporting Jackiw-Rebbi zero-mode is t_{JR}. The transmission coefficient between the two leads T_{12} depending on the incident electron's energy E as well as the magnetic flux ϕ inclosed [ϕ is in the unit of $\phi_0/(2\pi)$, ϕ_0 is the flux quantum] can be numerically investigated by the Green's function. For weak t_d [Fig. 2(b-d)], the AB effect shows an unexpected π-period sinusoidal oscillation in the zero-energy case that the incident electron's energy E matches the zero-mode's energy level. As E slightly

deviates from zero, T_{12} becomes the superposition of a π-period and a 2π-period sinusoidal functions. The AB effect comes back to the normal 2π-period sinusoidal oscillation for significant non-zero E. For strong t_d [Fig. 2(e-g)], though no longer in the simple sinusoidal form, the AB effect still exhibits a π-period oscillation for $E = 0$, while a 2π-period oscillation for $E \neq 0$.

The S-matrix theory [38,39] shows that T_{12} has the analytical form as:

$$T_{12} = \frac{4\tilde{t}_d^2 \cdot \tilde{E}^2 + 4\tilde{t}_d \cos\phi \cdot \tilde{E} + 1}{\left[\left(1 + \tilde{t}_d^2\right)\tilde{E} + \tilde{t}_d \cos\phi\right]^2 + 1}, \quad (2)$$

where $\tilde{t}_d \equiv \frac{t_d}{2v_f}$, and $\tilde{E} \equiv \frac{v_f}{t_0^2}(E - \epsilon_0)$ (see Supplementary Material). In the resonant tunneling condition $\tilde{E} = 0$, T_{12} reduces to $1/(\tilde{t}_d^2 \cos^2\phi + 1)$ thus verifies the π-period AB oscillation. Furthermore, the numerical results can be well fitted by Equation (2) (see Supplementary Material). In the limit of $\tilde{t}_d \to 0$, $T_{12} = 1/(\tilde{E}^2 + 1)$ indicates the transmission solely induced by the Jackiw-Rebbi zero-mode has a peak value of 1, other than the naively expected $1/2$. Such analytic result drawn from S-matrix is numerically verified [Fig. 2(h)] and consistent with previous research [18].

For comparison, if the Jackiw-Rebbi zero-mode in the AB ring is replaced by a MZM [40,41], then the transmission conductance G_{12} between the two leads is related to the S-matrix in the Bogoliubov-de Gennes basis [38,42] as

$$G_{12} = \frac{e^2}{h} \cdot \left\{\left|S_{12}^{ee}\right|^2 - \left|S_{12}^{he}\right|^2\right\}$$
$$= \frac{e^2}{h} \cdot \frac{-32\tilde{t}_d \sin\phi + 8\tilde{t}_d\left(1 - \tilde{t}_d^2\right)\cos\phi \cdot \tilde{E} + 4\tilde{t}_d^2\left(1 + \tilde{t}_d^2\right) \cdot \tilde{E}^2}{\left(1 + \tilde{t}_d^2\right) \cdot \left[16 + \left(1 + \tilde{t}_d^2\right)^2 \tilde{E}^2\right]}, \quad (3)$$

where $1, 2$ for lead indices, e, h for electron and hole, respectively, $\tilde{t}_d \equiv \frac{t_d}{2v_f}$, and $\tilde{E} \equiv \frac{2v_f}{t_M^2} E$ (see Supplementary Material). In contrast to the Jackiw-Rebbi zero-mode, Equation (3) indicates that MZM's AB effect oscillates in a 2π-period at both zero-bias ($\tilde{E} = 0$) and finite-bias ($\tilde{E} \neq 0$) [40]. However, as discussed above, Jackiw-Rebbi zero-mode can be viewed as a special case of MZM where PH symmetry is absent. The electron and hole indices in Equation (3) are replaced by two electron subband indices (denoted by α and β) if the Majorana condition is not imposed. Hence the sign difference between electron and hole is absent, and Equation (3) is modified as $G_{12} = \frac{e^2}{h}\{|S_{12}^{\alpha\alpha}|^2 + |S_{12}^{\beta\alpha}|^2\} = \frac{e^2}{h} \frac{16}{16 + (1 + \tilde{t}_d^2)^2 \cdot \tilde{E}^2} \cdot \{\frac{1}{2} + \frac{\tilde{t}_d^2}{(1 + \tilde{t}_d^2)^2} + \frac{\tilde{t}_d^2}{4}\tilde{E}^2 + \frac{\tilde{t}_d}{2}\frac{1 - \tilde{t}_d^2}{1 + \tilde{t}_d^2}\cos\phi \cdot \tilde{E} - \frac{\tilde{t}_d^2}{(1 + \tilde{t}_d^2)^2}\cos 2\phi\}$, which qualitatively retrieve the consequence that the Jackiw-Rebbi
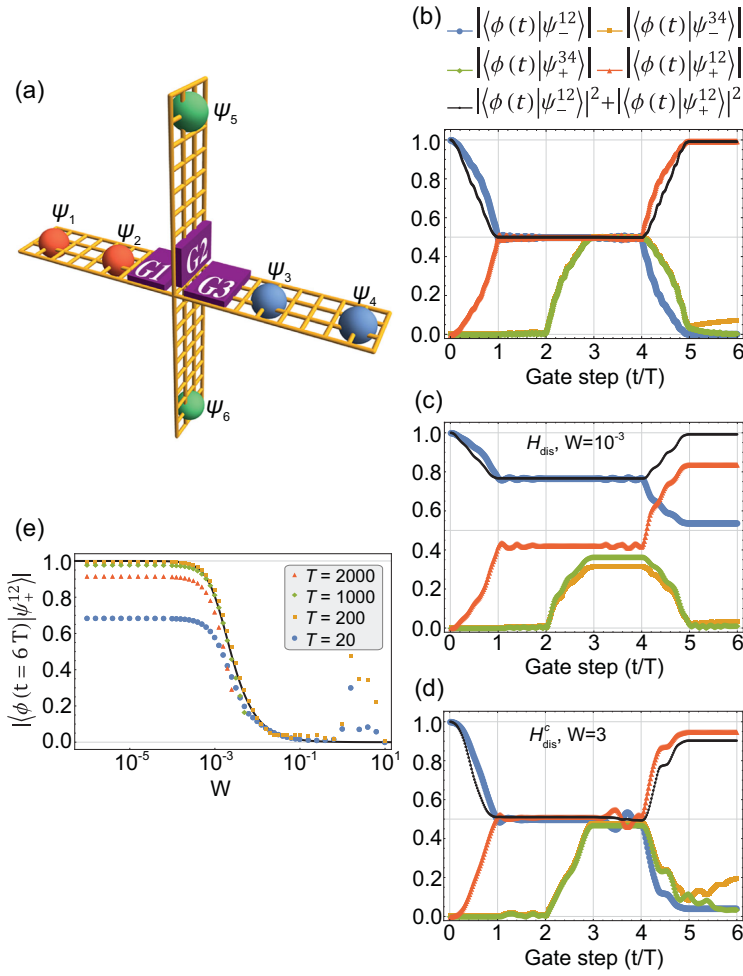
Figure 3. (a) Sketch of the cross-shaped QSHI junction. Distributions of the three pairs of Jackiw-Rebbi zero-modes ($\psi_{i=1,2,...,6}$) before braiding are shown. (b-d) Evolution of an eigenstate $\phi(t)$ as ψ_2 and ψ_3 are swapped twice in succession with $T = 200$ (b) in the clean limit; (c) in the presence of chiral-symmetry-breaking disorder $H_{\rm dis}$ with $W = 10^{-3}$; (d) in the presence of chiral-symmetry-conserved disorder $H_{\rm dis}^{C}$ with $W = 3$. $|\langle\phi(t = 6T)|\psi_{-}^{12}\rangle|^2 + |\langle\phi(t = 6T)|\psi_{+}^{12}\rangle|^2 = 1$ is valid in (b) and (c), while invalid in (d) for strong disorder destroying topological gap. (e) $|\langle\phi(t = 6T)|\psi_{+}^{12}\rangle|$ in a fixed chiral-symmetry-breaking disorder profile with different disorder strength W and braiding time T. Numerical results can be well fitted (black curve) by Equation (5) as $|\langle\phi(t = 6T)|\psi_{+}^{12}\rangle| = 1/(\tilde{\Delta}_{12}^2 + 1)^{1/2}$ for intermediate T satisfying adiabatic condition $\Delta_b \gg 1/T \gg \epsilon_{12},\epsilon_{34}$. Topological gap $\Delta_b \approx 0.2$, the coupling energy ϵ_{12}, $\epsilon_{34} \approx 7 \times 10^{-5}$.

zero-mode exhibits π-period (2π-period) AB effect at zero-bias (finite-bias).

NON-ABELIAN BRAIDING PROPERTIES

The similarities between Jackiw-Rebbi and MZM revealed by the AB effect inspire us to investigate the possible non-Abelian statistics of Jackiw-Rebbi zero-modes through cross-shaped junction [Fig. 3(a)]. Each of the four arms of the junction is a topologically nontrivial QSHI supporting Jackiw-Rebbi zero-

modes, and three gates (G1, G2, and G3) are located near the crossing. If the gate voltage is turned on (off), then the corresponding arm is separated (connected) due to the presence (absence) of the gating potential barrier. Initially, G1 and G3 are turned on while G2 is turned off, hence three pairs of Jackiw-Rebbi zero-modes (ψ_1, ψ_2, ... ψ_6) are localized at the ends of the three divided parts [Fig. 3(a)]. The braiding protocol [31] takes three steps (time cost for each step is T) to swap ψ_2 and ψ_3 spatially. Firstly, G1 is turned off and then G2 is turned on, hence ψ_2 is moved to the top of G2. Secondly, G3 is turned off and then G1 is turned on, so now ψ_3 is at the left of G1. Thirdly, turning off G2 is followed by turning on G3, as a result ψ_2 and ψ_3 are swapped. In the whole braiding process taking time of $2 \times 3T$, ψ_2 and ψ_3 are swapped twice in succession.

In the following, we verify that swapping ψ_2 and ψ_3 once lead to $\psi_2 \to \psi_3$ and $\psi_3 \to -\psi_2$, which is identical to the MZM [26,43]. In the clean limit, finite-size induced coupling betweem paired Jackiw-Rebbi zero-modes $\epsilon_{2i-1,2i}\, e^{i\alpha_{2i-1,2i}}\psi_{2i-1}^{\dagger}\psi_{2i} + h.c.$ ($i = 1, 2, 3$, and $\alpha_{2i-1,2i}$ for arbitrary phase) leads to symmetric and antisymmetric eigenstates $\psi_{\pm}^{12} = \frac{1}{\sqrt{2}}(\psi_1 \pm e^{-i\alpha_{12}}\psi_2)$ [16]. Numerical simulation of the adiabatic time-evolution (see Supplementary Material) shows that an eigenstate $\phi(t)$ evolving from ψ_{-}^{12} to ψ_{+}^{12} after ψ_2 and ψ_3 are swapped twice in succession [Fig. 3(b)], which indicates $\psi_2 \to -\psi_2$. Similarly, $\psi_3 \to -\psi_3$ is confirmed for another eigenstate evolving from ψ_{-}^{34} to ψ_{+}^{34} simultaneously. Consequently, braiding properties $\psi_2 \to \psi_3$ and $\psi_3 \to -\psi_2$ (after swapping ψ_2 and ψ_3 once) can be drawn from the above results up to a gauge transformation. It is worth noting that the basis of the wavefunction we adopted here is $(|\psi_{-}^{12}\rangle, |\psi_{-}^{34}\rangle, |\psi_{+}^{34}\rangle, |\psi_{+}^{12}\rangle)$ [Fig. 3(b)], while the basis usually chosen for MZMs' braiding is $(|0\rangle, \Psi_1^{\dagger}|0\rangle, \Psi_2^{\dagger}|0\rangle, \Psi_1^{\dagger}\Psi_2^{\dagger}|0\rangle)$ [26,31,32] instead.

GENERALIZED NON-ABELIAN BRAIDING IN SYSTEMS WITH DEGENERACY LIFTING

The QSHI constriction [Equation (1)] is in the AIII symmetry class possessing chiral symmetry $-H_{\rm QSHI}(-\mathbf{p}) = C\,H_{\rm QSHI}(\mathbf{p})C^{-1}$ [44,45], which protects the degeneracy of Jackiw-Rebbi zero-modes ($C = \pi_y\,\sigma_y$, π_y is Pauli matrix for real spin). Strikingly, the eigenstate $\phi(t)$ evolves from ψ_{12}^{-} to a superposition of ψ_{12}^{-} and ψ_{12}^{+} [Fig. 3(c)] in the presence of tiny chiral-symmetry-breaking disorder $H_{\rm dis} = {\rm diag}\{V_1(\mathbf{r}),\ V_2(\mathbf{r}),\ V_3(\mathbf{r}),\ V_4(\mathbf{r})\}$ ($V_i(\mathbf{r})$

uniformly distributed within $[-W/2, W/2]$) where disorder strength W comparable with ϵ_{12}, ϵ_{34} but much smaller than the topological gap Δ_b. On the contrary, the non-Abelian braiding remains integrity until the disorder is strong enough to destruct the topological gap [Fig. 3(d)], if the disorder has a chiral-symmetry-conserved form as $H_{\text{dis}}^C = \text{diag}\{V_1(\mathbf{r}), V_2(\mathbf{r}), -V_2(\mathbf{r}), -V_1(\mathbf{r})\}$ (see Supplementary Material).

Due to the self-conjugation condition $\gamma_i^\dagger = \gamma_i$, MZM's occupation energy term $\gamma_i^\dagger \gamma_i = 1$ is a trivial constant. For Jackiw-Rebbi zero-mode, however, $\psi_i^\dagger \neq \psi_i$ and the energy deviation $\Delta_{2i-1,2i} \psi_i^\dagger \psi_i$ (e.g., originated from disorder effect or gate voltages tuning local chemical potential) can be introduced into the Hamiltonian as:

$$H_{\text{JR}} = \Delta_{12} \psi_1^\dagger \psi_1 - \Delta_{12} \psi_2^\dagger \psi_2 + \Delta_{34} \psi_3^\dagger \psi_3$$
$$- \Delta_{34} \psi_4^\dagger \psi_4 + \Big(\epsilon_{12} e^{i\alpha_{12}} \psi_1^\dagger \psi_2$$
$$+ \epsilon_{34} e^{i\alpha_{34}} \psi_4^\dagger \psi_3 + h.c. \Big) \quad (4)$$

(widely separated zero-modes ψ_5 and ψ_6 with negligible coupling are dropped). The eigenstates of Equation (4) spanned by $|\psi_1\rangle$ and $|\psi_2\rangle$ are $\psi_\pm^{12} = \frac{1}{\sqrt{2}C_{12}^\pm} \{\psi_1 + e^{-i\alpha_{12}}[\pm(\tilde{\Delta}_{12}^2 + 1)^{1/2} - \tilde{\Delta}_{12}]\psi_2\}$ ($\tilde{\Delta}_{12} \equiv \Delta_{12}/\epsilon_{12}$, and $C_{12}^\pm$ are normalization constants). In case of non-zero Δ_{12}, numerical simulation confirms that the exchange properties $\psi_2 \to \psi_3$ and $\psi_3 \to -\psi_2$ are still valid (see Supplementary Material). However, due to the new form of eigenstates $\psi_\pm^{12}$ with different weights of ψ_1 and ψ_2 (in other words, $\tilde{\Delta}_{12}$ induces a 'rotation' of the eigenstates $\psi_\pm^{12}$), a novel non-Abelian braiding is obtained:

$$|\phi(t = 6T)\rangle = -\sin\delta \cdot |\psi_-^{12}\rangle + \cos\delta \cdot |\psi_+^{12}\rangle, \quad (5)$$

where $|\phi(t = 0)\rangle = |\psi_-^{12}\rangle$, and $\delta \in (-\pi/2, \pi/2)$ is defined as $\sin\delta \equiv \tilde{\Delta}_{12}/(\tilde{\Delta}_{12}^2 + 1)^{1/2}$ and $\cos\delta \equiv 1/(\tilde{\Delta}_{12}^2 + 1)^{1/2}$. With the increase of $|\delta|$ describing the degeneracy lifting, the $|\psi_-^{12}\rangle$ component in $|\phi(t = 6T)\rangle$ increases from 0 to 1, while the weight of $|\psi_+^{12}\rangle$ decreases from 1 to 0. In the adiabatic condition $\Delta_b \gg 1/T \gg \epsilon_{12}$, ϵ_{34} [31], numerical simulation results are T-independent and well fitted by Equation (5) [Fig. 3(e)]. According to the model described above, if moderate coupling strength $\epsilon_{2i-1,2i}$ between Jackiw-Rebbi zero-modes is provided, δ will be relatively small for weak disorder and therefore the non-Abelian braiding properties identical to the MZMs can be retrieved.

Table 1. Braiding operator $B = F^{-1} R^2 F$, fusion operator F, and the square of exchange operator R for both Jackiw-Rebbi zero-mode and MZM. θ_B is an overall phase factor.

Operator	Jackiw-Rebbi zero-mode	MZM
B	$e^{-i\theta_B} \begin{pmatrix} -\sin\delta & \cos\delta \\ \cos\delta & \sin\delta \end{pmatrix}$	$e^{-i\frac{\pi}{4}} \begin{pmatrix} 0 & 1 \\ 1 & 0 \end{pmatrix}$
F	$\begin{pmatrix} -\sin(\frac{\delta}{2} - \frac{\pi}{4}) & \cos(\frac{\delta}{2} - \frac{\pi}{4}) \\ \cos(\frac{\delta}{2} - \frac{\pi}{4}) & \sin(\frac{\delta}{2} - \frac{\pi}{4}) \end{pmatrix}$	$\frac{1}{\sqrt{2}} \begin{pmatrix} 1 & 1 \\ 1 & -1 \end{pmatrix}$
R^2	$e^{-i\theta_B} \begin{pmatrix} 1 & 0 \\ 0 & -1 \end{pmatrix}$	$e^{-i\frac{\pi}{4}} \begin{pmatrix} 1 & 0 \\ 0 & -1 \end{pmatrix}$

Furthermore, by exerting additional gate voltages modulating the local chemical potentials of ψ_1 and ψ_4, δ and then the non-Abelian braiding properties can be modulated in a controlled manner. For chiral-symmetry-conserved disorder H_{dis}^C, in contrast, disorders in opposite signs are imposed on edge states with opposite chirality, hence the energy deviation $\Delta_{12} = 0$ and the corresponding non-Abelian properties remain the same as the MZM.

Mathematically, in the basis of $\{|\psi_1, \psi_2; \psi_-^{12}\rangle, |\psi_1, \psi_2; \psi_+^{12}\rangle\}$ (where $|\psi_1, \psi_2; \psi_\pm^{12}\rangle$ indicating ψ_1 and ψ_2 fusing into $\psi_\pm^{12}$), as shown in Table 1, such novel braiding can be expressed in the form of braiding operator B [46,47]. Besides, the fusion operator F and the exchange operator R can also be extracted from $B = F^{-1} R^2 F$ (see Supplementary Material). The fusion rule of Jackiw-Rebbi zero-mode can be tuned by δ and is a generalization of MZM (Table 1). In the limit of $\delta = 0$, as expected, it retrieves MZM's fusion rule up to a phase θ_B. Such generalized and tunable fusion rule implies potential application in topological quantum computation.

Finally, if 'fictitious' PH-symmetry-breaking disorder is introduced into a $p \pm ip$-wave superconductor (D symmetry class [48,49]), then similar δ-dependent braidings are also observed for MZM (see Supplementary Material). The only difference is that the important role preserving MZMs' degeneracy is played by PH symmetry instead of chiral symmetry.

DISCUSSIONS

The relation and similarity between Jackiw-Rebbi and MZM are uncovered by both AB effect and non-Abelian braiding properties. Though the double-frequency AB oscillation of the Jackiw-Rebbi zero-mode is irrelevant to the charge fractionalization,

such effect relies on the resonant condition $\tilde{E} = 0$ in which Jackiw-Rebbi zero-mode's zero-energy nature is topologically protected, while such peculiarity can be easily removed for an ordinary zero-mode such as a localized state in a quantum dot. As for the non-Abelian properties, the symmetry-protected degeneracy for MZM is robust since PH symmetry is always presented provided that the superconductivity is not destroyed, therefore the fusion rule of MZM has a fixed form while the Jackiw-Rebbi one is tunable. Furthermore, for MZM-based braiding, considering the adiabatic condition ϵ_{12}, $\epsilon_{34} \ll 1/T \ll \Delta_b$ [31] where the SC gap Δ_b is in the order of 1 meV, it requires relative low braiding frequency $1/T$ and larger device scale to reduce the finite-size-induced coupling ϵ_{12}, ϵ_{34}. These restrictions could be relaxed for Jackiw-Rebbi zero-modes since superconductivity is no longer required and the topological gap Δ_b could be generally larger. These comparisons show the possibility of quantum computation device with higher integration level and higher braiding frequency.

SUPPLEMENTARY DATA

Supplementary data are available at *NSR* online.

ACKNOWLEDGEMENTS

FUNDING

REFERENCES

1. Jackiw R and Rebbi C. Solitons with fermion number 1/2. *Phys Rev D* 1976; **13**: 3398–409.
2. Goldstone J and Wilczek F. Fractional quantum numbers on solitons. *Phys Rev Lett* 1981; **47**: 986–9.
3. Kivelson S and Schrieffer JR. Fractional charge, a sharp quantum observable. *Phys Rev B* 1982; **25**: 6447–51.
4. Rajaraman R and Bell JS. On solitons with half integral charge. *Phys Lett B* 1982; **116**: 151–4.
5. Rajaraman R. Fractional charge. arXiv:cond-mat/0103366.
6. Jackiw R. Fractional and Majorana fermions: the physics of zero-energy modes. *Phys Scr* 2012; **T146**: 014005.
7. Laughlin RB. Nobel lecture: fractional quantization. *Rev Mod Phys* 1999; **71**: 863–74.
8. Seidel A and Lee D-H. Abelian and non-abelian Hall liquids and charge-density wave: quantum number fractionalization in one and two dimensions. *Phys Rev Lett* 2006; **97**: 056804.
9. Arovas D, Schrieffer JR and Wilczek F. Fractional statistics and the quantum Hall effect. *Phys Rev Lett* 1984; **53**: 722–3.
10. Lee D-H, Zhang G-M and Xiang T. Edge solitons of topological insulators and fractionalized quasiparticles in two dimensions. *Phys Rev Lett* 2007; **99**: 196805.
11. Ruostekoski J, Dunne GV and Javanainen J. Particle number fractionalization of an atomic Fermi-Dirac gas in an optical lattice. *Phys Rev Lett* 2002; **88**: 180401.
12. Shen S-Q. *Topological Insulators*. Berlin: Springer, 2012.
13. Su WP, Schrieffer JR and Heeger AJ. Solitons in polyacetylene. *Phys Rev Lett* 1979; **42**: 1698–701.
14. Kitaev AY. Unpaired Majorana fermions in quantum wires. *Phys-Usp* 2001; **44**: 131–6.
15. Tewari S, Das Sarma S and Lee D-H. Index theorem for the zero modes of Majorana fermion vortices in chiral *p*-Wave superconductors. *Phys Rev Lett* 2007; **99**: 037001.
16. Klinovaja J and Loss D. Fractional fermions with non-Abelian statistics. *Phys Rev Lett* 2013; **110**: 126402.
17. Pedrocchi FL, Chesi S and Gangadharaiah S *et al.* Majorana states in inhomogeneous spin ladders. *Phys Rev B* 2012; **86**: 205412.
18. Rainis D, Saha A and Klinovaja J *et al.* Transport signatures of fractional fermions in Rashba nanowires. *Phys Rev Lett* 2014; **112**: 196803.
19. Klinovaja J, Stano P and Loss D. Transition from fractional to Majorana fermions in Rashba nanowires. *Phys Rev Lett* 2012; **109**: 236801.
20. Klinovaja J and Loss D. Fermionic and Majorana bound states in hybrid nanowires with non-uniform spin-orbit interaction. *Eur Phys J B* 2015; **88**: 62.
21. Gangadharaiah S, Trifunovic L and Loss D. Localized end states in density modulated quantum wires and rings. *Phys Rev Lett* 2012; **108**: 136803.
22. Klinovaja J and Loss D. Fractional charge and spin states in topological insulator constrictions. *Phys Rev B* 2015; **92**: 121410.
23. Väyrynen JI and Ojanen T. Chiral topological phases and fractional domain wall excitations in one-dimensional chains and wires. *Phys Rev Lett* 2011; **107**: 166804.
24. Qi X-L, Hughes TL and Zhang S-C. Fractional charge and quantized current in the quantum spin Hall state. *Nat Phys* 2008; **4**: 273–6.
25. Halperin BI, Oreg Y and Stern A *et al.* Adiabatic manipulations of Majorana fermions in a three-dimensional network of quantum wires. *Phys Rev B* 2012; **85**: 144501.
26. Ivanov DA. Non-Abelian statistics of half-quantum vortices in *p*-wave superconductors. *Phys Rev Lett* 2001; **86**: 268–71.
27. Alicea J, Oreg Y and Refael G *et al.* Non-Abelian statistics and topological quantum information processing in 1D wire networks. *Nat Phys* 2011; **7**: 412–7.

28. Sau JD, Clarke DJ and Tewari S. Controlling non-Abelian statistics of Majorana fermions in semiconductor nanowires. *Phys Rev B* 2011; **84**: 094505.

29. Gao P, He Y-P and Liu X-J. Symmetry-protected non-Abelian braiding of Majorana Kramers pairs. *Phys Rev B* 2016; **94**: 224509.

30. Sekania M, Plugge S and Greiter M *et al.* Braiding errors in interacting Majorana quantum wires. *Phys Rev B* 2017; **96**: 094307.

31. Amorim CS, Ebihara K and Yamakage A *et al.* Majorana braiding dynamics in nanowires. *Phys Rev B* 2015; **91**: 174305.

32. Chen C-Z, Xie Y-M and Liu J *et al.* Quasi-one-dimensional quantum anomalous Hall systems as new platforms for scalable topological quantum computation. *Phys Rev B* 2018; **97**: 104504.

33. Saha A, Rainis D and Tiwari RP *et al.* Quantum charge pumping through fractional fermions in charge density modulated quantum wires and Rashba nanowires. *Phys Rev B* 2014; **90**: 035422.

34. Fu H, Wu Y and Zhang R *et al.* 3/2 fractional quantum Hall plateau in confined two-dimensional electron gas. *Nat Commun* 2019; **10**: 4351.

35. Bernevig BA, Hughes TL and Zhang S-C. Quantum spin Hall effect and topological phase transition in HgTe quantum wells. *Science* 2006; **314**: 1757–61.

36. Qi X-L and Zhang S-C. Topological insulators and superconductors. *Rev Mod Phys* 2011; **83**: 1057–110.

37. Heeger AJ, Kivelson S and Schrieffer JR *et al.* Solitons in conducting polymers. *Rev Mod Phys* 1988; **60**: 781–850.

38. Law KT, Lee PA and Ng TK. Majorana fermion induced resonant andreev reflection. *Phys Rev Lett* 2009; **103**: 237001.

39. Datta S. *Electronic Transport in Mesoscopic Systems.* Cambridge: Cambridge University Press, 1997.

40. Tripathi KM, Das S and Rao S. Fingerprints of Majorana bound states in Aharonov-Bohm geometry. *Phys Rev Lett* 2016; **116**: 166401.

41. Benjamin C and Pachos JK. Detecting Majorana bound states. *Phys Rev B* 2010; **81**: 085101.

42. Nilsson J, Akhmerov AR and Beenakker CWJ. Splitting of a cooper pair by a pair of Majorana bound states. *Phys Rev Lett* 2008; **101**: 120403.

43. von Oppen F, Peng Y and Pientka F. Topological superconducting phases in one dimension. Oxford: Oxford University Press, 2015.

44. Altland A and Zirnbauer MR. Nonstandard symmetry classes in mesoscopic normal-superconducting hybrid structures. *Phys Rev B* 1997; **55**: 1142–61.

45. Schnyder AP, Ryu S and Furusaki A *et al.* Classification of topological insulators and superconductors in three spatial dimensions. *Phys Rev B* 2008; **78**: 195125.

46. Lahtinen V and Pachos JK. A short introduction to topological quantum computation. *SciPost Phys* 2017; **3**: 021.

47. Pachos JK. *Introduction to Topological Quantum Computation.* Cambridge: Cambridge University Press, 2012.

48. Lin Y, Hao W and Wang M *et al.* Topological superconductors from one-dimensional periodically modulated Majorana chains. *Sci Rep* 2017; **7**: 9210.

49. Bernevig BA and Hughes TL. *Topological Insulators and Topological Superconductors.* Princeton: Princeton University Press, 2013.